MATHEMATICAL BIOSCIENCES
AND ENGINEERING
Volume **8**, Number **2**, April **2011**

doi:10.3934/mbe.2011.8.425

pp. **425–443**

BLOOD COAGULATION DYNAMICS: MATHEMATICAL MODELING AND STABILITY RESULTS

Adélia Sequeira

Department of Mathematics and CEMAT/IST
Instituto Superior Técnico
Technical University of Lisbon
Av. Rovisco Pais 1, 1049-001 Lisboa, Portugal

Rafael F. Santos

Department of Mathematics and CEMAT/IST
Faculty of Sciences and Technology
University of Algarve
Campus de Gambelas 8005-139 Faro, Portugal

Tomáš Bodnár

Department of Technical Mathematics
Faculty of Mechanical Engineering
Czech Technical University
Náměstí 13, 121 35 Prague 2, Czech Republic

Abstract. The hemostatic system is a highly complex multicomponent biosystem that under normal physiologic conditions maintains the fluidity of blood. Coagulation is initiated in response to endothelial surface vascular injury or certain biochemical stimuli, by the exposure of plasma to Tissue Factor (TF), that activates platelets and the coagulation cascade, inducing clot formation, growth and lysis. In recent years considerable advances have contributed to understand this highly complex process and some mathematical and numerical models have been developed. However, mathematical models that are both rigorous and comprehensive in terms of meaningful experimental data, are not available yet. In this paper a mathematical model of coagulation and fibrinolysis in flowing blood that integrates biochemical, physiologic and rheological factors, is revisited. Three-dimensional numerical simulations are performed in an idealized stenosed blood vessel where clot formation and growth are initialized through appropriate boundary conditions on a prescribed region of the vessel wall. Stability results are obtained for a simplified version of the clot model in quiescent plasma, involving some of the most relevant enzymatic reactions that follow Michaelis-Menten kinetics, and having a continuum of equilibria.

1. **Introduction.** When a blood vessel is injured, a complex physiologic process characterized by interactions between the vessel wall, platelets, coagulation factors and their inhibitors and fibrinolytic proteins, is set into action. This process, called hemostasis, leads to the formation of a solid fibrin clot to cover the vascular lesion and to stop hemorrhage. It includes several steps: (1) vasoconstriction, to reduce

2000 *Mathematics Subject Classification.* Primary: 76Z05, 92B05, 34D15, 34D20, 37B25, 93D99; Secondary: 76M12.

Key words and phrases. Blood coagulation, clot growth, continuum of equilibria, semistability.

blood input and loss in the damaged region; (2) primary hemostasis, induced by platelets activation in contact with collagen exposed by arterial damage, resulting in the formation of a hemostatic plug within seconds after the injury. Platelets can also be activated and form aggregates by prolonged exposure to sharp or rapid increases in shear stress [8]; (3) secondary hemostasis or coagulation, a complex cascade of enzymatic reactions involving coagulation factors, down to the production of Thrombin which converts Fibrinogen into Fibrin, stabilizing the platelet plugs and forming a blood clot (or thrombus). It has two pathways, intrinsic and extrinsic, which join in a common pathway leading to Fibrin production; (4) wall repair: the clot attracts and stimulates the growth of fibroblasts and smooth muscle cells, repairing the vessel wall; (5) clot dissolution (or clot lysis), leading to the restoration of normal blood flow conditions, at the end of the hemostatic process.

Blood clots are continuously produced and dissolved inside blood vessels. However, some abnormal hemodynamic and biochemical conditions can lead to severe pathologies such as bleeding or thromboembolic disorders. In the last case, clots can detach to form an embolus which can lodge in a smaller vessel downstream from the site of thrombosis, induce ischemia of the irrigated tissues, and result in a stroke, heart attack or pulmonary embolism.

The process of blood clotting produced by the mechanical activation of platelets combined with a biochemical cascade of kinetic reactions, is quite complex and not yet well understood. Experimental studies recognize that clot formation and growth primarily occur in stagnation flow regions, within blood vessel bifurcations, branching, strong curvatures or severe stenoses. Moreover, internal cardiovascular devices such as prosthetic heart valves, ventricular assist devices and stents, generally harbor high hemodynamic shear stresses that can cause platelet activation and result in clot formation. Thrombotic deposition is a major cause of failure of those medical devices.

In recent years considerable advances have contributed to understand this highly complex process. Reviews describing the blood coagulation system are available (see, e.g. [1], [14]) but comprehensive mathematical models have been lacking in general. Most models have focused only on biochemical systems, others incorporate some fluid mechanical factors but not the mechanical properties of blood and the forming clots [3], [9], [16]. Moreover, these models rely on experimental data obtained from reductionist in vitro experiments and with little physiological relevance.

Anand et al. [1] recently developed a mathematical model for clot formation and lysis in flowing blood that attempts to extend existing models, to integrate more of the biochemical, physiologic and rheological factors, but it is yet far from being complete. Preliminary 3D numerical results for a simplified version of this model, where the viscoelasticity of blood is not considered, can be found in [5].

Numerical simulations motivated the need to better understand the behavior of this mathematical model. In particular, problems of chemical stability and equilibria have gained high importance. From the physiological point of view, clot formation generally occurs due to specific perturbations in the hemostatic system. However, under normal, undisturbed conditions, biochemical constituents of blood are in a kind of chemical equilibrium and thus no coagulation processes take place. Normal concentrations of the biochemical species seem also to be equilibrium solutions of the coagulation system, in the sense that, if they are slightly perturbed, they tend to revert back to their equilibrium (normal) values. Therefore, in view

of these considerations, the stability analysis of the biochemical system becomes mandatory.

This paper is mainly devoted to the study of stability of equilibria of some of the most relevant enzymatic reactions involved in the biochemical part of the model analyzed in [5]. It is organized as follows. The coupled problem is formulated in Sect. 2 and results of the 3D numerical simulations performed in an idealized stenosed vessel are presented in Sect. 3. Finally, preliminary stability results can be found in Sect. 4 and the paper ends with some concluding remarks.

2. **Formulation of the mathematical model.** We briefly recall the coupled blood flow - biochemistry model of clot growth and lysis studied in [5].

It is assumed that the flow of blood is governed by the equations for an incompressible generalized Newtonian fluid with shear-thinning viscosity

$$\begin{aligned} \rho\left(\frac{\partial \mathbf{u}}{\partial t}+\mathbf{u}\cdot\nabla\mathbf{u}\right) &= -\nabla p+\operatorname{div}\tau(\mathbf{u}) \\ \operatorname{div}\mathbf{u} &= \mathbf{0} \end{aligned} \tag{1}$$

completed with appropriate initial and boundary conditions. In these equations, defined in a three-dimensional domain Ω, $\mathbf{u}(x,t)$ is the velocity field, $p(x,t)$ is the pressure, ρ is the fluid density and $\tau(\mathbf{u})$ is the deviatoric stress tensor. This tensor defined by

$$\tau(\mathbf{u}) = \mathbf{2}\mu(\dot{\gamma})\mathbf{D} \tag{2}$$

and is proportional to the symmetric part of the velocity gradient $\mathbf{D} = (\nabla\mathbf{u} + \nabla\mathbf{u}^T)/2$, $\dot{\gamma} = 2\sqrt{\mathbf{D}:\mathbf{D}}$ is the shear rate (a measure of the rate of shear deformation) and $\mu(\dot{\gamma})$ is the shear dependent viscosity function inversely related to the shear rate.

Here, we consider the generalized Cross model to account for the shear-thinning behavior of blood. The corresponding viscosity function is written as

$$\frac{\mu(\dot{\gamma})-\mu_\infty}{\mu_0-\mu_\infty} = \frac{1}{(1+(\lambda\dot{\gamma})^b)^a} \tag{3}$$

where μ_0 and μ_∞ are the asymptotic viscosities at low and high shear rates and parameters λ, a and b are estimated by curve fitting of experimental data (see [13]). In particular we take $\mu_0 = 1.6\cdot 10^{-1}\mathrm{Pa}\cdot\mathrm{s}$, $\mu_\infty = 3.6\cdot 10^{-3}\mathrm{Pa}\cdot\mathrm{s}$, $a = 1.23, b = 0.64$ and $\lambda = 8.2\mathrm{s}$, from [10].

To simulate the cascade of biochemical reactions involved in the coagulation process, a system of 23 coupled advection-diffusion-reaction equations is used. It describes the evolution in time and space of various enzymes and zymogenes, proteins, inhibitors, Tissue Plasminogen Activator and Fibrin/Fibrinogen (see Table 1) leading to the formation, growth and dissolution of clots in quiescent plasma. It is based on the model introduced in [1] and further developed in [2] (see also [5]), as already mentioned.

This system takes the form

$$\frac{\partial[\mathsf{C}_i]}{\partial t} + \operatorname{div}\left([\mathsf{C}_i]\,\mathbf{u}\right) = \operatorname{div}\left(\mathsf{D}_i\nabla[\mathsf{C}_i]\right) + \mathsf{R}_i \qquad i = 1,\dots,23 \tag{4}$$

where $[\mathsf{C}_i]$ represents the concentration of the $i-$th constituent, D_i denotes the diffusion coefficient associated with C_i and $\mathbf{u}$ is the velocity field. The nonlinear reaction terms that represent the production or depletion of C_i due to the enzymatic

cascade of reactions are represented by R_i and their specific form is shown in Table 2, which also contains the diffusion coefficients, obtained from experiments, (see [1], [2] and references cited therein). Some of the reactions follow Michaelis-Menten kinetics and others follow first order or second order kinetics.

Species	Names	Species	Names
IXa	Factor IXa	XIa	Factor XIa
IX	Factor IX	XI	Factor XI
$VIIIa$	Factor VIIIa	$ATIII$	AntiThrombin-III
$VIII$	Factor VIII	$TFPI$	Tissue Factor Pathway Inhibitor
Va	Factor Va	APC	Active Protein C
V	Factor V	PC	Protein C
Xa	Factor Xa	$L1AT$	α_1-AntiTrypsin
X	Factor X	tPA	Tissue Plasminogen Activator
IIa	Thrombin	PLA	Plasmin
II	Prothrombin	PLS	Plasminogen
Ia	Fibrin	$L2AP$	α_2-AntiPlasmin
I	Fibrinogen	Z	Tenase
		W	Prothrombinase

TABLE 1. Constituents involved in the coagulation cascade and fibrinolysis

Equations (4) are complemented with appropriate initial and flux boundary conditions involving the concentration of various species at an injured site of the vascular wall.

Initially there is no clot. Coagulation starts by the exposure of blood to Tissue Factor (TF-VIIa complex), released from sub-endothelium in an injured region of the vessel wall. Tissue Factor binds Factor VIIa and activates factors IX and X. Once Factor Xa is generated, the coagulation process develops and a clot is formed when Fibrin concentration [Ia] is equal or greater than a specific value in certain flow region located at the vicinity of the injured wall. When [Ia] drops below this value or a high shear stress forces clot's rupture, the repair process of the injury begins, resulting in fibrinolysis and clot dissolution.

We assume the same constitutive model for the blood and the clot, but we impose different viscosity values. A viscosity factor related to the Fibrin concentration around the injured vessel wall region is introduced such that, it is equal to 1 when Fibrin concentration is close to zero and the local viscosity is equal to the viscosity of blood. As the Fibrin concentration grows, the viscosity increases linearly up to a certain threshold C_{Clot} and the viscosity factor is equal to μ^*. The parameters μ^* and C_{clot} should be chosen to mimic the clot properties. In our study we have used $\mu^* = 100$ and $\mathsf{C}_{Clot} = 1000\ nM$ corresponding to a viscosity of the clot region 100 times higher than that of the blood.

This empirical assumption based on a Fibrin concentration viscosity factor makes reasonable predictions but should be improved if additional constituents and their interactions are incorporated in the biochemical model.

3. **Numerical simulations and results.** The governing equations for the coupled blood-biochemistry model (1) - (4) have been solved using a finite volume

Species	Reaction Terms	Diffusion Coeff. $[cm^2/s]$
IXa	$\frac{k_9[XIa][IX]}{K_{9M}+[IX]} - h_9[IXa][ATIII]$	6.27×10^{-7}
IX	$-\frac{k_9[XIa][IX]}{K_{9M}+[IX]}$	5.63×10^{-7}
$VIIIa$	$\frac{k_8[IIa][VIII]}{K_{8M}+[VIII]} - h_8[VIIIa] - \frac{h_{C8}[APC][VIIIa]}{H_{C8}+[VIIIa]}$	3.92×10^{-7}
$VIII$	$-\frac{k_8[IIa][VIII]}{K_{8M}+[VIII]}$	3.12×10^{-7}
Va	$\frac{k_5[IIa][V]}{K_{5M}+[V]} - h_5[Va] - \frac{h_{C5}[APC][Va]}{H_{C5M}+[Va]}$	3.82×10^{-7}
V	$-\frac{k_5[IIa][V]}{K_{5M}+[V]}$	5.63×10^{-7}
Xa	$\frac{k_{10}[Z][X]}{K_{10M}+[X]} - h_{10}[Xa][ATIII] - h_{TFPI}[TFPI][Xa]$	7.37×10^{-7}
X	$-\frac{k_{10}[Z][X]}{K_{10M}+[X]}$	5.63×10^{-7}
IIa	$\frac{k_2[W][II]}{K_{2M}+[II]} - h_2[IIa][ATIII]$	6.47×10^{-7}
II	$-\frac{k_2[W][II]}{K_{2M}+[II]}$	5.21×10^{-7}
Ia	$\frac{k_1[IIa][I]}{K_{1M}+[I]} - \frac{h_1[PLA][Ia]}{H_{1M}+[Ia]}$	2.47×10^{-7}
I	$-\frac{k_1[IIa][I]}{K_{1M}+[I]}$	3.10×10^{-7}
XIa	$\frac{k_{11}[IIa][XI]}{K_{11M}+[XI]} - h_{11}^{A3}[XIa][ATIII] - h_{11}^{L1}[XIa][L1AT]$	5.00×10^{-7}
XI	$-\frac{k_{11}[IIa][XI]}{K_{11M}+[XI]}$	3.97×10^{-7}
$ATIII$	$-(h_9[IXa] + h_{10}[Xa] + h_2[IIa] + h_{11}^{A3}[XIa])[ATIII]$	5.57×10^{-7}
$TFPI$	$-h_{TFPI}[TFPI][Xa]$	6.30×10^{-7}
APC	$\frac{k_{PC}[IIa][PC]}{K_{PCM}+[PC]} - h_{PC}[APC][L1AT]$	5.50×10^{-7}
PC	$-\frac{k_{PC}[IIa][PC]}{K_{PCM}+[PC]}$	5.44×10^{-7}
$L1AT$	$-h_{PC}[APC][L1AT] - h_{11}^{L1}[XIa][L1AT]$	5.82×10^{-7}
tPA	0	5.28×10^{-7}
PLA	$\frac{k_{PLA}[tPA][PLS]}{K_{PLAM}+[PLS]} - h_{PLA}[PLA][L2AP]$	4.93×10^{-7}
PLS	$-\frac{k_{PLA}[tPA][PLS]}{K_{PLAM}+[PLS]}$	4.81×10^{-7}
$L2AP$	$-h_{PLA}[PLA][L2AP]$	5.25×10^{-7}
Z	$[Z] = \frac{[VIIIa][IXa]}{K_{dZ}}$	0.0^*
W	$[W] = \frac{[Va][Xa]}{K_{dW}}$	0.0^*

TABLE 2. Reaction terms and diffusion coefficients

space-discretization on structured grids, and an explicit multistage Runge-Kutta time integration scheme. To avoid numerical oscillations a pressure stabilization technique has been implemented. We look for steady solutions by a time-marching approach, i.e. the unsteady governing systems are solved with steady boundary conditions and stationary solutions are recovered when t tends to infinity. At each time step an iterative process is used to couple the flow and the biochemical solutions. First, the velocity field is computed using equations (1) with a given viscosity, and is inserted into (4) to obtain the concentrations (including that of Fibrin). Next, the local viscosity is updated by a factor which depends on the calculated Fibrin concentration in the clotting area (as described above), and the flow field is recomputed in the next time step using the updated viscosity (see [5] for further details).

Numerical simulations have been performed in an idealized non-symmetric (with respect to the bulk flow direction) cosine-shaped stenosed vessel. The vessel is assumed to be three-dimensional, axisymmetric, rigid-walled, with circular cross-section, and with length $L = 10R = 31mm$ and diameter $D = 2R = 6.2mm$ (see Fig. 1 (a)). The diameter is reduced to one half in the stenosed region, which leads to a $4 : 1$ cross-sectional area reduction and thus to a significant speed-up of the local flow.

A parabolic velocity profile is prescribed at the inlet, with flow rate $Q = 2\ cm^3 s^{-1}$, while at the outlet flow is assumed to be fully developed, i.e. homogeneous Neumann conditions are imposed for the velocity components and the pressure is fixed to a constant. On the vessel walls no-slip Dirichlet conditions are used for the velocity field. Moreover, homogeneous Neumann boundary conditions for the concentrations of all the chemical species are imposed at the healthy vessel wall. To simulate the wall injury, non-homogeneous Neumann conditions for seven selected species, directly involved in the initiation of the coagulation cascade $(IXa, IX, Xa, X, XIa, XI, tPa)$, are imposed in that region [5].

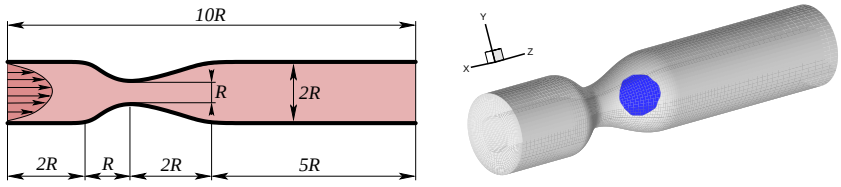

(a) stenosis (b) vessel wall initial injury

FIGURE 1. Computational domain

Physiological values have been used as initial conditions for the concentrations of the biochemical species. These values can be found in the literature, except those of the activated species [1], [2]. Theoretically, the lowest values could initially be considered equal to zero. However, to avoid numerical instabilities, we were compelled to take non zero values and considered a 0.1% initial activation. The initial conditions actually used are listed in Table 3, (see also [1], [2] and [5]).

The computational domain was discretized using a structured, wall fitted mesh with hexahedral cells. To avoid high distortion of cells, a multiblock mesh structure was adopted, with an outer mesh block of $64 \times 16 \times 1100$ cells and a central mesh block of $16 \times 16 \times 110$ control volumes.

Species	Initial values $[nM]$	Species	Initial values $[nM]$
IXa	0.09	XIa	0.03
IX	90.0	XI	30.0
$VIIIa$	0.0007	$ATIII$	2410.0
$VIII$	0.7	$TFPI$	2.5
Va	0.02	APC	0.06
V	20.0	PC	60.0
Xa	0.17	$L1AT$	45000.0
X	170.0	tPA	0.08
IIa	1.4	PLA	2.18
II	1400.0	PLS	2180.0
Ia	7.0	$L2AP$	105.0
I	7000.0		

TABLE 3. Initial concentrations

The center of the simulated clotting area was placed at the wall vessel, $4R$ from the inlet. The clotting surface was considered inside a sphere of diameter R. The location of the wall injury was chosen in a region of stagnant or recirculation flow, downstream the stenosis, where thrombosis can occur (see Fig. 1 (b)).

The concentrations of all chemical species involved in the model have been computed pointwise in the whole computational domain. Figure 2 illustrates the evolution in time ($600s$) of the concentrations of some of the most important species in the center of the clotting surface. In particular, we observe a jump in all these concentrations, approximately $100s$ after the initiation of the clotting cascade and a rapid increase of Fibrin concentration, with a maximum value attained approximately at $150s$, remaining relatively stable after that time. Moreover, results shown in Fig. 2 also suggest that in the clotting process, ATIII deficiency is more relevant than PC deficiency, as observed in [1], in a similar situation.

Cloth growth on the vessel wall after 600 seconds, based on the significant increase of Fibrin concentration in the clotting area, is shown in Fig. 3. The blood flow direction is from left to right. Due to advection Fibrin is transported downstream the injured vessel wall region and during the clotting process the shape of the clot is changed. In these simulations we could also observe the first steps of clot dissolution, in regions where Fibrin concentration starts to decrease.

Figure 4 shows flow deceleration caused by the increase of Fibrin concentration. Flow velocity reduces in the clot area due to the enhancement of local viscosity. The blue region indicates low flow speed, while red areas correspond to high speed undisturbed flow.

It is natural to assume that concentrations of chemicals transported by blood do not vary in time. This state could be called a chemical equilibrium and equilibria concentrations, or some close values, could be used as initial conditions. (Note that values close to those in Table 3 give results similar to the ones shown in Fig. 2). This and what was referred earlier concerning the 0.1% initial activation, motivated the need for studying the stability of the system, which is done in a particular setting, in Sect. 4.2.

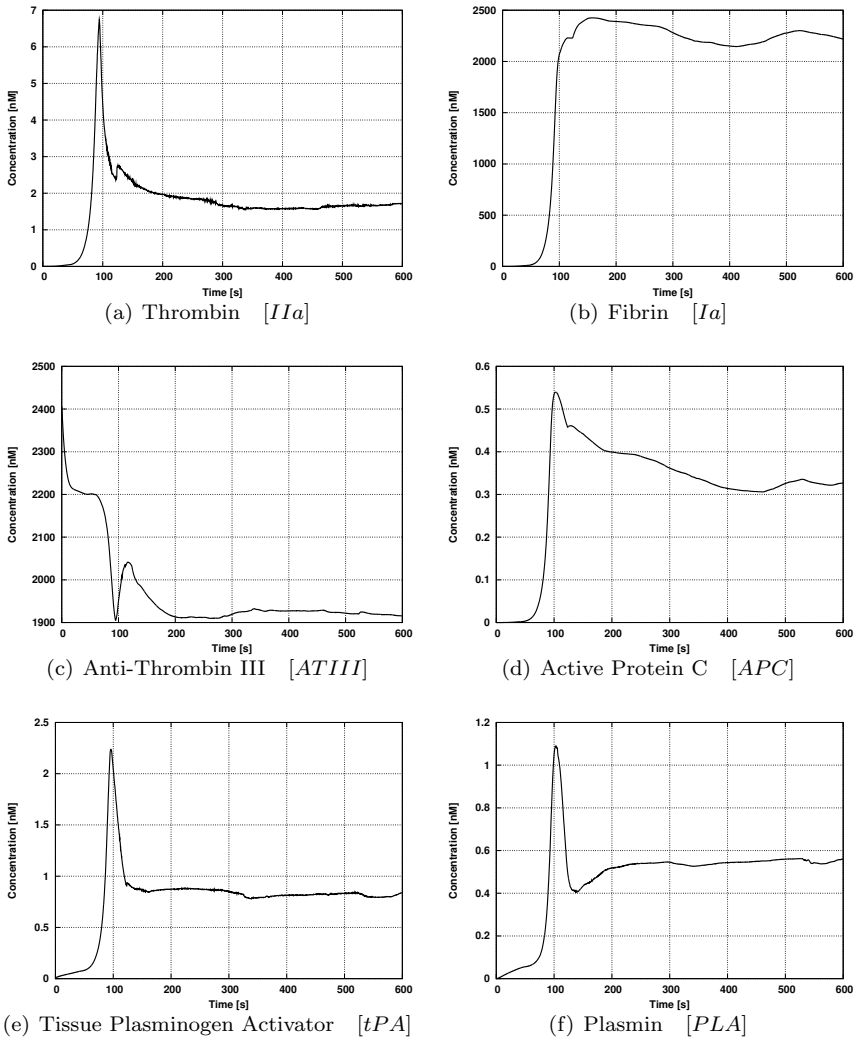

(a) Thrombin $[IIa]$ (b) Fibrin $[Ia]$

(c) Anti-Thrombin III $[ATIII]$ (d) Active Protein C $[APC]$

(e) Tissue Plasminogen Activator $[tPA]$ (f) Plasmin $[PLA]$

FIGURE 2. Time evolution of selected concentrations in the center of clotting surface.

A related issue is the fact that reaction terms representing second order or Michaelis-Menten approximations will be equal to zero unless both species involved have non vanishing concentrations. Therefore, if one concentration is perturbed on the boundary and the other (activated) is initiated to zero the process of coagulation will not be able to start. In Sect. 4.1 we establish a result relating kinetic equations and Michaelis-Menten approximations, which also shows how initial data to the two systems relate to each other. Since the full problem is a (coupled) multiscale problem, this is also a way to understand the relationship between initial values of activated and non activated species.

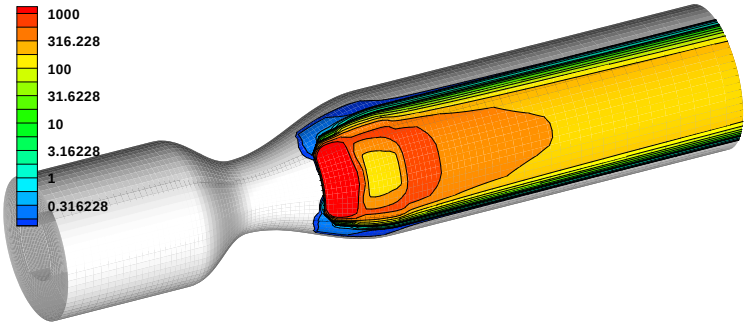

FIGURE 3. Fibrin concentration on the vessel surface after 600 seconds

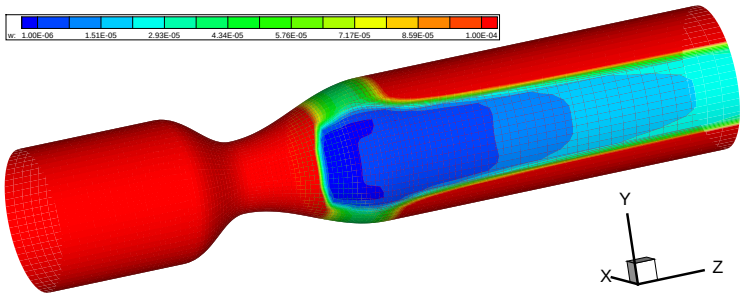

FIGURE 4. Axial velocity in the near-wall layer after 600 seconds

4. **Stability of the coagulation model in quiescent plasma.**

4.1. **Equations governing the biochemical cascade.** The coagulation cascade described by equations (4) include several chemical reactions that are assumed to follow first order, second order and Michaelis-Menten kinetics. We briefly recall how Michaelis-Menten approximations are obtained from a set of kinetic equations [11].

Consider a chemical reaction

$$\mathrm{S} + \mathrm{E} \underset{k_{-1}}{\overset{k_1}{\rightleftharpoons}} \mathrm{C} \xrightarrow{k_2} \mathrm{E} + \mathrm{P},$$

where a substrate S reacts with an enzyme E. The result of this reaction is, irreversibly, a product P and the enzyme E. Meanwhile, reversibly, a complex C is formed. By mass action laws we know that concentrations are solutions of the

following system of ordinary differential equations:

$$\begin{aligned}
\frac{d}{dt}[S] &= -k_1\,[S]\,[E] + k_{-1}\,[C], && (5)\\
\frac{d}{dt}[E] &= -k_1\,[S]\,[E] + (k_{-1}+k_2)\,[C], && (6)\\
\frac{d}{dt}[C] &= k_1\,[S]\,[E] - (k_{-1}+k_2)\,[C], && (7)\\
\frac{d}{dt}[P] &= k_2\,[C], && (8)
\end{aligned}$$

along with the initial conditions

$$[S](0) = [S_0], \qquad [E](0) = [E_0], \qquad [C](0) = [C_0], \qquad [P](0) = [P_0],$$

where $[X]$ denotes the concentration of X, and k_1, k_{-1} and k_2 are rate constants for the association of the substrate S and the enzyme E, the dissociation of (unaltered) substrate from the enzyme and the dissociation of the product from the enzyme, respectively.

By adding equations (6) and (7) it follows that $E(t)+C(t)$ is a constant in time, that is $E(t)+C(t) = E_0$. This allows to reduce system (5)-(8) to the system formed by equation (8) and

$$\begin{aligned}
\frac{d}{dt}[S] &= -k_1\,[S]\,([E_0]-[C]) + k_{-1}\,[C], && (9)\\
\frac{d}{dt}[C] &= k_1\,[S]\,([E_0]-[C]) - (k_{-1}+k_2)\,[C]. && (10)
\end{aligned}$$

We now make the so called *quasi-steady-state assumption*: the rate of the overall reaction, that is, the rate of formation of the product, $\frac{d}{dt}[P]$, is almost constant. Therefore C is also "almost constant", from which it follows that $\frac{d}{dt}[C] \approx 0$.

Defining the Michaelis-Menten constant, K_M, by $K_M = \frac{k_{-1}+k_2}{k_1}$, the quasi-steady-state assumption implies

$$[C] \approx \frac{[E_0]\,[S]}{K_M + [S]}. \tag{11}$$

Going back to equation (9), we find that

$$\frac{d[S]}{dt} \approx -\frac{k_2\,[E_0]\,[S]}{K_M + [S]}. \tag{12}$$

which is the well known Michaelis-Menten approximation.

Observe now that the product reaction rate can be obtained as

$$\frac{d}{dt}[P] \approx \frac{k_2\,[E_0]\,[S]}{K_M + [S]}.$$

Remark 1. If E is continuously supplied in time, then

$$\begin{aligned}
\frac{d[S]}{dt} &\approx -\frac{k_2\,[E]\,[S]}{K_M + [S]},\\
\frac{d}{dt}[P] &\approx \frac{k_2\,[E]\,[S]}{K_M + [S]},
\end{aligned}$$

which is the form encountered in the reaction terms of system (4).

We now recall, following [15], how Michaelis-Menten approximation can be obtained as the solution to a singular perturbation problem. We first introduce the following scaled dimensionless variables

$$s = [S]/[S_0]; \qquad c = [C]/\frac{[E_0][S_0]}{K_M + [S_0]}; \qquad T = t/\frac{k_2\,[E_0]}{K_M + [S_0]};$$

and also define the parameters

$$\sigma = [S_0]/K_M; \qquad k = k_{-1}/k_2; \qquad \epsilon = \frac{[E_0]}{K_M + [E_0]},$$

with $0 < \epsilon << 1$ (see e.g. [5]).

The dimensionless form of equations (9)-(10) is then given by

$$\frac{ds^\epsilon}{dT} = (k+1)(\sigma+1)\left[-s^\epsilon + \frac{\sigma}{\sigma+1}c^\epsilon s^\epsilon + \frac{k(k+1)^{-1}}{\sigma+1}c^\epsilon\right], \tag{13}$$

$$\epsilon\frac{dc^\epsilon}{dT} = (k+1)(\sigma+1)\left[s^\epsilon - \frac{\sigma}{\sigma+1}c^\epsilon s^\epsilon - \frac{1}{\sigma+1}c^\epsilon\right]. \tag{14}$$

Problem (13)-(14) is a singular perturbation problem. The solution of a singular perturbation problem of this type consists in general, of two parts: one initial layer, whose size decreases exponentially with time and an interior solution "in the large", that is, after the dying out of the initial layer part of the solution. Here, we are interested in the interior solution. It is sought in the form

$$s^\epsilon(T) = s_0(T) + \epsilon s_1(T) + \epsilon^2 s_2(T) + \cdots, \tag{15}$$

$$c^\epsilon(T) = c_0(T) + \epsilon c_1(T) + \epsilon^2 c_2(T) + \cdots. \tag{16}$$

Inserting (15) and (16) into (13) and (14) and equating like powers of ϵ, we find, at order zero, that c_0 and s_0 should verify

$$c_0(T) = \frac{(\sigma+1)s_0(T)}{\sigma s_0(T) + 1}, \tag{17}$$

$$\frac{ds_0}{dT}(T) = -\frac{(\sigma+1)s_0(T)}{\sigma s_0(T) + 1}, \tag{18}$$

the last equation being the dimensionless form of equation (12). Note that, in the reaction terms of the blood coagulation system (4) (see Table 2) only the approximations of order zero appear, that is, in dimensionless form, s_0 and c_0. As usual, $f = O(\epsilon)$ if there exists a positive constant C such that $|f| \leq C\epsilon$. We have the following theorem:

Theorem 4.1. *Let $s_0(0) = s_{0,0}$ and $s_1(0) = s_{1,0}$ be such that $s^\epsilon(0) = s_{0,0} + \epsilon s_{1,0} + g^\epsilon$, with $g^\epsilon = O(\epsilon)$; let s_0, for $T \in [0, T_1]$, be the solution of (18) and let c_0 be given by (17). Let also s_1 be the solution of*

$$\frac{ds_1}{dT} = -(k+1)\left[\sigma + 1 - \sigma c_0(T)\right] s_1(T), \quad T \in [0, T_1]. \tag{19}$$

Then there exists a constant $C > 0$ such that $s^\epsilon(T) = s_0(T) + \omega^\epsilon(T)$ with $|\omega^\epsilon| \leq C\epsilon$.

Remark 2. Note that the solution of (18) lies in a compact set, $[0, a]$, without leaving it. Therefore, $T_1 = +\infty$.

Proof. We first simplify equations (13) and (14) and write them as

$$\frac{ds^\epsilon}{dT} = -(k+1)\left[\sigma+1-\sigma c^\epsilon\right]s^\epsilon + kc^\epsilon \tag{20}$$

$$\epsilon\frac{dc^\epsilon}{dT} = (k+1)\left[\left(\sigma+1-\sigma c^\epsilon\right)s^\epsilon - c^\epsilon\right] \tag{21}$$

We write $c^\epsilon = c_0$, $s^\epsilon = s_0 + \epsilon s_1 + \omega^\epsilon$ and insert these expressions in equation (20) to obtain

$$\begin{aligned}\frac{ds_0}{dT} + \epsilon\frac{ds_1}{dT} + \frac{d\omega^\epsilon}{dT} &= -(k+1)\left[\sigma+1-\sigma c_0\right](s_0+\epsilon\, s_1+\omega^\epsilon) + kc_0 \qquad (22)\\ &= -(k+1)\left[\sigma+1-\sigma c_0\right]s_0 + kc_0\\ &- \epsilon\,(k+1)\left[\sigma+1-\sigma c_0\right]\,s_1\\ &- (k+1)\left[\sigma+1-\sigma c_0\right]\,\omega^\epsilon \qquad (23)\end{aligned}$$

and in equation (21) to obtain

$$\begin{aligned}\epsilon\frac{dc_0}{dT} &= (k+1)\left[\left(\sigma+1-\sigma c_0\right)s_0 - c_0\right] \qquad (24)\\ &+ \epsilon\,(k+1)\left[\sigma+1-\sigma c_0\right]\,s_1\\ &+ (k+1)\left[\sigma+1-\sigma c_0\right]\,\omega^\epsilon\end{aligned}$$

Now, taking into account (17)-(19), we deduce from (23)-(24) that ω^ϵ is the solution of

$$\frac{d\omega^\epsilon}{dT} = -\epsilon\left(\frac{ds_0}{dT}+\frac{ds_1}{dT}\right) \tag{25}$$

$$\omega^\epsilon(0) = g^\epsilon \tag{26}$$

Since the right hand sides of (18) and (19) both satisfy Lipschitz conditions, and $g^\epsilon = O(\epsilon)$, the conclusion follows. □

4.2. **Continuum of equilibria and stability.** To solve numerically the system of partial differential equations for the blood coagulation model, it is important to impose good initial data, that could, for example, represent well mixed blood. This can be considered by neglecting fluid velocity and the (very small) diffusion coefficients. If we want to deal with more realistic situations, we could consider medical data as well. In either case, as already referred (end of Sect. 3), a stability analysis of the resulting system becomes mandatory. Neglecting fluid velocity and diffusion coefficients leads to a system of ordinary differential equations and good initial data should be an equilibrium solution to that system. (Remember that y is an *equilibrium solution* to $y'(t) = f(y(t))$ if $y'(t) = 0$, that is, equilibria are the zeros of f). In this case, the ODE system is as follows:

$$\begin{cases}\frac{d[IX_a]}{dt} = \frac{k_9\,[XI_a][IX]}{K_{9M}+[IX]} - h_9\,[IX_a]\,[ATIII]\\ \frac{d[IX]}{dt} = -\frac{k_9\,[XI_a][IX]}{K_{9M}+[IX]}\end{cases} \tag{27}$$

$$\begin{cases}\frac{d[VIII_a]}{dt} = \frac{k_8\,[II_a]\,[VIII]}{K_{8M}+[VIII]} - h_8\,[VIII_a] - \frac{h_{c8}\,[APC]\,[VIII_a]}{H_{c8M}+[VIII_a]}\\ \frac{d[VIII]}{dt} = -\frac{k_8\,[II_a]\,[VIII]}{K_{8M}+[VIII]}\end{cases} \tag{28}$$

$$\begin{cases}\frac{d[V_a]}{dt} = \frac{k_5\,[II_a]\,[V]}{K_{5M}+[V]} - h_5\,[V_a] - \frac{h_{c5}\,[APC]\,[V_a]}{H_{c5M}+[V_a]}\\ \frac{d[V]}{dt} = -\frac{k_5\,[II_a]\,[V]}{K_{5M}+[V]}\end{cases} \tag{29}$$

$$\begin{cases} \frac{d[X_a]}{dt} &= \frac{k_{10}\,[Z]\,[X]}{K_{10M}+[X]} - h_{10}\,[X_a][ATIII] - h_{TFPI}[TFPI][X_a] \\ \frac{d[X]}{dt} &= -\frac{k_{10}\,[Z]\,[X]}{K_{10M}+[X]} \end{cases} \tag{30}$$

$$\begin{cases} \frac{d[II_a]}{dt} &= \frac{k_2\,[W]\,[II]}{K_{2M}+[II]} - h_2\,[II_a]\,[ATIII] \\ \frac{d[II]}{dt} &= -\frac{k_2\,[W]\,[II]}{K_{2M}+[II]} \end{cases} \tag{31}$$

$$\begin{cases} \frac{d[I_a]}{dt} &= \frac{k_1\,[II_a]\,[I]}{K_{1M}+[I]} - \frac{h_1\,[PLA]\,[I_a]}{H_{1M}+[I_a]} \\ \frac{d[I]}{dt} &= -\frac{k_1\,[II_a]\,[I]}{K_{1M}+[I]} \end{cases} \tag{32}$$

$$\begin{cases} \frac{d[XI_a]}{dt} &= \frac{k_{11}\,[II_a]\,[XI]}{K_{11M}+[XI]} - h_{11}^{A3}[XI_a][ATIII] - h_{11}^{L1}[XI_a][L1AT] \\ \frac{d[XI]}{dt} &= -\frac{k_{11}\,[II_a]\,[XI]}{K_{11M}+[XI]} \end{cases} \tag{33}$$

$$\begin{cases} \dfrac{d[ATIII]}{dt} = -\left(h_9[IX_a] + h_{10}[X_a] + h_2[II_a] + h_{11}^{A3}[XI_a]\right)[ATIII] \end{cases} \tag{34}$$

$$\begin{cases} \dfrac{d[TFPI]}{dt} = -h_{TFPI}[TFPI][X_a] \end{cases} \tag{35}$$

$$\begin{cases} \frac{d[APC]}{dt} &= \frac{k_{PC}\,[II_a]\,[PC]}{K_{PCM}+[PC]} - h_{PC}[APC][L1AT] \\ \frac{d[PC]}{dt} &= -\frac{k_{PC}\,[II_a]\,[PC]}{K_{PCM}+[PC]} \end{cases} \tag{36}$$

$$\begin{cases} \dfrac{d[L1AT]}{dt} = -h_{PC}[APC][L1AT] - h_{11}^{L1}[XI_a][L1AT] \end{cases} \tag{37}$$

$$\begin{cases} \dfrac{d[tPA]}{dt} = 0 \end{cases} \tag{38}$$

$$\begin{cases} \frac{d[PLA]}{dt} &= \frac{k_{PLA}\,[tPA]\,[PLS]}{K_{PLAM}+[PLS]} - h_{PLA}[PLA][L2AP] \\ \frac{d[PLS]}{dt} &= -\frac{k_{PLA}\,[tPA]\,[PLS]}{K_{PLAM}+[PLS]} \end{cases} \tag{39}$$

$$\begin{cases} \dfrac{d[L2AP]}{dt} = -h_{PLA}[PLA][L2AP] \end{cases} \tag{40}$$

Equilibria for this system are the solutions to the following equations:

$$\begin{array}{lcllcl} [XIa]\,[IX] &=& 0, & [IXa]\,[ATIII] &=& 0, \\ [IIa]\,[VIII] &=& 0, & [VIIIa] &=& 0, \\ [IIa]\,[V] &=& 0, & [Va] &=& 0, \\ [Z]\,[X] &=& 0, & [Xa]\,[ATIII] &=& 0, \\ [Xa]\,[TFPI] &=& 0, & [W]\,[II] &=& 0, \end{array} \tag{41}$$

$$\begin{array}{lcllcl} [IIa]\,[ATIII] &=& 0, & [IIa]\,[I] &=& 0, \\ [PLA]\,[Ia] &=& 0, & [IIa]\,[XI] &=& 0, \\ [XIa]\,[ATIII] &=& 0, & [XIa]\,[L1AT] &=& 0, \\ [IIa]\,[PC] &=& 0, & [APC]\,[L1AT] &=& 0, \\ [tPA]\,[PLS] &=& 0, & [PLA]\,[L2AP] &=& 0. \end{array} \tag{42}$$

By solving system (41)-(42) we are able to show that system (27)-(40) has a continuum of equilibrium points. This is a feature, common to several non negative dynamical systems, that complicates its stability analysis and, in these cases, semistability has to be called for.

The zero solution is an obvious equilibrium solution. But there are many other configurations of equilibria. Moreover, if we solve the system above we find that there are non isolated equilibria. Continuum of equilibria are common to nonnegative dynamical systems as well as to compartmental dynamical systems. The blood coagulation system, modeling a cascade of biochemical reactions, is an example of a nonnegative compartmental system. For a continuum of equilibria, asymptotic stability must be ruled out since in every neighborhood of an equilibrium point there exists a different one. In this case, the concept of *semistability* should be used. Semistability was introduced for the first time in [7] and requires that solution curves converge to limit points that are Lyapunov stable. Since semistability is much less known than classical stability, we briefly recall its main definitions and results, following [4].

Let

$$y'(t) = f(y(t)), \tag{43}$$

where $f : \mathcal{D} :\to \mathbb{R}^n$ is continuous on the open set $\mathcal{D} \subset \mathbb{R}^n$.

Definition 4.2. Given $x \in \mathcal{D}$, the orbit $\mathcal{O}_x$ of x is the set $\{\psi(t, x) : t \geq 0\}$, where $\psi(t, x)$ is the solution of (43) starting from the initial condition $y(0) = x$.

Definition 4.3. A set $\mathcal{G}$ is positively invariant (under f) if $\psi(t, x) \in \mathcal{G}$, for all $x \in \mathcal{G}$ and $t \geq 0$.

Let $\mathcal{G} \subset \mathcal{D}$ be a locally compact, positively invariant set such that $\mathcal{O}_x \subset \mathcal{G}$, for all $x \in \mathcal{G}$.

Definition 4.4. A set $\mathcal{U} \subset \mathcal{G}$ is relatively bounded in $\mathcal{G}$ if $\overline{\mathcal{U}}$ is a compact subset of $\mathcal{G}$.

The following is a definition of *derivative along a solution* of (43):

Definition 4.5. Given $V : \mathcal{G} :\to \mathbb{R}^n$,

$$\dot{V}(x) = \lim_{t \to 0^+} \frac{1}{t} \left\{ V(\psi(t, x)) - V(x) \right\}.$$

Definition 4.6. A function $\mathcal{U} : \mathcal{G} \to \mathbb{R}$ is proper if $\mathcal{U}^{-1}(K)$ is a compact set in $\mathcal{G}$, for all compact $K \subset \mathbb{R}$.

Proposition 1. *If there exists a continuous, proper function $U : \mathcal{G} :\to \mathbb{R}$ such that $\dot{U}$ is defined on $\mathcal{G}$, $U \geq 0$ and $\dot{U}(x) \leq 0$, for all $x \in \mathcal{G}$, then $\mathcal{O}_x$ is relatively bounded on $\mathcal{G}$, for every $x \in \mathcal{G}$.*

For a given $K \subset \mathbb{R}^n$, we denote by $coco(K)$ the cone generated by the union of the convex hulls of the connected components of K.

Definition 4.7. The direction cone $\mathcal{F}_x$ of f at x, relatively to $\mathcal{G}$, is the intersection of all sets $\overline{coco(f(\mathcal{U}) \setminus \{0\})}$, where $\mathcal{U} \subset \mathcal{G}$ is an open neighborhood of x in $\mathcal{G}$.

A generalization of a tangent space is provided by the tangent cone. Let $x \in K \subset \mathbb{R}^n$.

Definition 4.8. (i) A vector $v \in \mathbb{R}^n$ is tangent to K, at x, if there exists a sequence $\{x_i\} \subset K$ and a sequence $h_i \to 0$ such that

$$\lim_{t \to +\infty} \frac{1}{h_i} (x_i - x) = v.$$

(ii) The tangent cone to K at x is the closed cone, $T_x K$, of all vectors tangent to K at x.

This implies that the vector field f is nontangent to $K \subset \mathcal{G}$, at $x \in K$, if $T_x K \cap \mathcal{F}_x \subset \{0\}$.

Direction cones are not easy to determine in applications. Instead, we make use of the limiting direction set of f. First, let $\mathcal{E}$ be the set of equilibria of (43). For $x \in \mathcal{G} \backslash \mathcal{E}$, a vector $v \in S^{n-1}$ is a limiting direction of f at x if there exists $\{x_i\} \subset \mathcal{G} \backslash \mathcal{E}$ such that $\lim_{i \to \infty} x_i = x$ and $\lim_{i \to \infty} \frac{1}{\|f(x_i)\|} f(x_i) = v$.

Definition 4.9. For $x \in \mathcal{G}$, the positive set of x relative to $\mathcal{G}$, $\mathcal{O}_x^\infty$, is the set of points $z \in \mathcal{G}$ such that there exists a divergent sequence $\{t_i\} \subset [0, \infty)$ with $\lim_{i \to \infty} \psi(t_i, x) = z$.

Proposition 2. *Let $x \in \mathcal{G}$. If $\mathcal{O}_x$ is relatively bounded in $\mathcal{G}$, then $\mathcal{O}_x^\infty$ is nonempty, compact, invariant, connected and $\psi(t, x) \to \mathcal{O}_x^\infty$, as $t \to \infty$; that is, for every open subset $\mathcal{U} \subset \mathcal{G}$ that contains $\mathcal{O}_x^\infty$, there exists $T > 0$ such that $\psi(t, x) \in \mathcal{U}$ for all $t > T$. Moreover, $\lim_{t \to \infty} \psi(t, x)$ exists and is contained in $\mathcal{G}$ if and only if $\mathcal{O}_x^\infty$ contains exactly one point.*

Proposition 3. *Let $x \in \mathcal{G}$ and suppose that $\mathcal{O}_x^\infty$ is nonempty. Then, $\lim_{t \to \infty} \psi(t, x)$ exists and is contained in $\mathcal{G}$ if and only if there exists $z \in \mathcal{O}_x^\infty$ such that f is nontangent to $\mathcal{O}_x^\infty$ at z, relative to $\mathcal{G}$.*

Proposition 4. *Suppose $V : \mathcal{G} :\to \mathbb{R}$ is a continuous function such that $\dot{V}$ is defined on $\mathcal{G}$ and $\dot{V}(x) \leq 0$, for all $x \in \mathcal{G}$. Let $x \in \mathcal{G}$ be such that $\mathcal{O}_x$ is relatively bounded in $\mathcal{G}$. Let $\mathcal{P}$ and $\mathcal{N}$ denote the largest invariant subsets of the sets $\{z \in \mathcal{G} : V(z) \leq V(x)\}$ and $\dot{V}^{-1}(0)$, respectively. Then $\mathcal{O}_x^\infty \subset \mathcal{P} \cap \mathcal{N}$. In addition, if $\dot{V} \equiv 0$, then $\mathcal{O}_x^\infty$ is contained in the largest invariant subset of $V^{-1}(V(x))$.*

Definition 4.10. An equilibrium point $x \in \mathcal{G}$ is semistable, relative to $\mathcal{G}$, if there exists an open neighborhood $\mathcal{U} \subset \mathcal{G}$, of x, such that if $z \in \mathcal{U}$ then $lim_{t \to \infty} \psi(t, z)$ exists and is Lyapunov stable.

Proposition 5. *Suppose $V : \mathcal{G} :\to \mathbb{R}$ is a continuous function such that $\dot{V}$ is defined on $\mathcal{G}$. Let $x \in \mathcal{E}$ be a local maximizer of $\dot{V}$ relative to $\mathcal{G}$ and a local minimizer of V relative to the set $K \equiv \mathcal{G} \backslash \overline{\dot{V}^{-1}(0)}$. Let $\mathcal{W} \subset \mathcal{G}$ be an open neighborhood of x. For every $z \in \mathcal{E} \cap \mathcal{W}$, let $\mathcal{M}_z$ denote the largest connected subset of $V^{-1}(V(z)) \cap \mathcal{W}$ that is negatively invariant and contains z. Let $\mathcal{N}$ denote the largest negatively invariant subset of $\overline{\dot{V}^{-1}(0)} \cap \mathcal{W}$ and, for every $z \in \mathcal{N}$, let $\mathcal{N}_z$ denote the connected component of $\mathcal{N}$ containing z.*

If there exists an open neighborhood $\mathcal{U} \subset \mathcal{W}$ of x such that every equilibrium in $\mathcal{U}$ is a local minimizer of V relative to K and, for every $z \in \mathcal{N} \cap \mathcal{U}$, f is nontangent to $\mathcal{N}_z$ at z relative to $\mathcal{G}$, then x is semistable relative to $\mathcal{G}$.

4.3. **Semistability of a simplified biochemical model.** We now show how one can prove semistability of equilibria. However, instead of considering the full coagulation system (27)-(40), we take a simplified one which deals with a small, but significant part of the coagulation cascade. In fact, we consider a system consisting of equations (31), (32), (39) and (40), slightly modified. A similar system has been considered in [6]. Although it does not include all blood species involved in the coagulation cascade, it still has the ability to model coagulation and lysis as well:

$$\frac{d[II_a]}{dt} = \frac{k_2\,[W]\,[II]}{K_{2M}+[II]} \tag{44}$$

$$\frac{d[II]}{dt} = -\frac{k_2\,[W]\,[II]}{K_{2M}+[II]} \tag{45}$$

$$\frac{d[I_a]}{dt} = \frac{k_1\,[II_a]\,[I]}{K_{1M}+[I]} - \frac{h_1\,[PLA]\,[I_a]}{H_{1M}+[I_a]} \tag{46}$$

$$\frac{d[I]}{dt} = -\frac{k_1\,[II_a]\,[I]}{K_{1M}+[I]} \tag{47}$$

$$\frac{d[PLA]}{dt} = \frac{k_{PLA}\,[tPA]\,[PLS]}{K_{PLAM}+[PLS]} - h_{PLA}[PLA][L2AP] \tag{48}$$

$$\frac{d[PLS]}{dt} = -\frac{k_{PLA}\,[tPA]\,[PLS]}{K_{PLAM}+[PLS]} \tag{49}$$

$$\frac{d[L2AP]}{dt} = -h_{PLA}[PLA][L2AP] \tag{50}$$

Like in [6], we also suppose that Prothrombinase concentration, $[W]$, is a given function of time only. For closing, we have neglected the action of Antithrombin-3 in equation (44). Besides Prothrombinase, the system involves Prothrombin, II, Thrombin, II_a, Fibrinogen, I, Fibrin, I_a, Plasminogen, PLS, Plasmin, PLA, α2-Antiplasmin, $L2AP$, and Tissue Plasminogen Activator, tPA (see Table 1). Note, however, that the first four equations are coupled with the last three equations through Plasmin concentration, $[PLA]$, only. With this in mind we will further simplify, by assuming that $[PLA]$ is a given function of time and consider the first four equations only.

Let $y = (y_1, y_2, y_3, y_4) \equiv ([II_a], [I_a], [II], [I])^T$. Then equations (44)-(47) can be written, in form (43), as

$$\frac{dy}{dt} = f(y) \equiv v_1 y_1 y_4 + v_2 y_2 + v_3 y_3 \tag{51}$$

with

$$v_1 = \begin{bmatrix} 0 \\ \frac{k_1}{(K_{1M}+[I])} \\ 0 \\ \frac{-k_1}{(K_{1M}+[I])} \end{bmatrix};\ v_2 = \begin{bmatrix} 0 \\ \frac{-h_1[PLA]}{(H_{1M}+[I_a])} \\ 0 \\ 0 \end{bmatrix};\ v_3 = \begin{bmatrix} \frac{k_2[W]}{(K_{2M}+[II])} \\ 0 \\ \frac{-k_2[W]}{(K_{2M}+[II])} \\ 0 \end{bmatrix}.$$

Let now $\mathcal{G} = \{x \in \mathbb{R}^4 : x_i \geq 0\}$. Note that set $\mathcal{G}$ is positively invariant, under the action of the vector field defined by (51).

Since vectors v_i, $i = 1, 2, 3$ are linearly independent, equilibria are the solutions to

$$\begin{cases} y_1\, y_4 &= 0, \\ y_2 &= 0, \\ y_3 &= 0. \end{cases}$$

so that the set $\mathcal{E}$, of equilibria, is $\mathcal{E} = \mathcal{E}_1 \cup \mathcal{E}_2$ with

$$\mathcal{E}_1 = \{y \in \mathcal{G} : y_2 = y_3 = y_4 = 0\}\,,$$
$$\mathcal{E}_2 = \{y \in \mathcal{G} : y_1 = y_2 = y_3 = 0\}\,.$$

In view of the definitions and results outlined in Sect. 4.2 (see also [4]) we conclude that f is nontangent to $\mathcal{E}_1$, in every point $x \in \mathcal{E}_1$. In fact, the direction cone $\mathcal{F}_x$ of f at any $x \in \mathcal{G}$ is contained in the span of $\{v_i\}_{i=1,\cdots,3}$. On the other hand, given $x \in \mathcal{E}_1$, every vector tangent to $\mathcal{E}_1$, at x, is contained in the span of $v_4 = [1\,0\,0\,0]^T$. Since

$$\text{span}\,\{v_1,\, v_2,\, v_3\} \cap \text{span}\,\{v_4\} = \{0\}\,, \tag{52}$$

then the tangent cone T_x satisfies $T_x\mathcal{E}_1 \cap \mathcal{F}_x \subset \{0\}$, for all $x \in \mathcal{E}_1$. Thus f is nontangent to $\mathcal{E}_1$, in every point $x \in \mathcal{E}_1$.

Now, we claim that every equilibrium point $x \in \mathcal{E}_1$ is semistable. For that we consider the following (Lyapunov candidate) function $V : \mathcal{G} \to \mathbb{R}$ defined by $V(x) = x_2 + x_3 + x_4$. We can see that $V(x) \geq 0$, for all $x \in \mathcal{G}$ and $V^{-1}(0) = \overline{\mathcal{E}_1}$ and, consequently, every point in $\mathcal{E}_1$ is a local minimizer of V, relative to $\mathcal{G}$. On the other hand,

$$\dot{V}(x) = -\frac{h_1[PLA]x_2}{H_{1M} + x_2} - \frac{k_2 W x_3}{K_{2M} + x_3}.$$

Therefore $\dot{V}(x) \leq 0$, for all $x \in \mathcal{G}$,

$$\dot{V}^{-1}(0) = \{x \in \mathcal{G} : x_2 = 0,\, x_3 = 0\}$$

and the largest negatively invariant subset of $\overline{\dot{V}^{-1}(0)}$ contains $\mathcal{E}$.

Let $x \in \mathcal{E}_1$. There exists a relatively open neighborhood $\mathcal{U} \subset \mathcal{G}$ such that $\mathcal{U} \cap \mathcal{E}_1 = \mathcal{U} \cap \mathcal{E}$. It follows that every $z \in \mathcal{U} \cap \mathcal{E}$ is a local maximizer of $\dot{V}$ and a local minimizer of V, relative to $\mathcal{G}$. Since f is nontangent to $\mathcal{E}$ at every $z \in \mathcal{U} \cap \mathcal{E}$, it follows, from Proposition 5, after taking $\mathcal{W} = \mathcal{G}$, that every equilibrium in $\mathcal{E}_1$ is semistable, relative to $\mathcal{G}$.

Remark 3. It is not possible to show semistability of equilibria for $\mathcal{E}_2$, using the previous approach. Hence, and to study equilibria of the complete system (27)-(40), a different technique should be used, for example constructing Lyapunov functions. This is the object of current research.

5. **Concluding remarks.** A mathematical model of coagulation and fibrinolysis in flowing blood that integrates biochemical, physiologic and rheological factors, based on a more complex model developed in [1], has been considered in this work. Three-dimensional numerical simulations have been performed in an idealized stenosed blood vessel, following first simulations of the same model detailed in [5].

Preliminary results on the stability analysis of the system of equations associated to the biochemical part of the previous model, simulating the cascade of enzymatic reactions involved in the formation, growth and lysis of clots in quiescent plasma, have also been obtained. In particular, using a nontangency-based Lyapunov criterion, we have shown semistability for the kinetics of some of the most relevant

Michaelis-Menten chemical reactions involved in the model, that have a continuum of equilibria. Equilibria studied here are non clotting, due to the fact that they represent (final) configurations where Fibrin is absent (see, for example, [12] for a similar situation).

Several additional constituents and their interactions involved in platelet activation and aggregation, such as von-Willebrand Factor (vWF) and others, can be incorporated to develop new models that capture more realistic features. We believe that a deep analysis of stability results for these systems can be used to gain a better understanding of hemostasis and its regulation.

Acknowledgments. This work has been partially supported by CEMAT/IST through the Funding Program of FCT and by Project PTDC/MAT/68166/2006. The third author is grateful to the Czech Science Foundation under the Grant No.201/09/0917, the Grant Agency of the Academy of Sciences of the CR under the Grant No. IAA100190804 and to the Research Plan MSM 6840770010 of the Ministry of Education of Czech Republic.

REFERENCES

[1] M. Anand, K. Rajagopal and K. R. Rajagopal, *A model incorporating some of the mechanical and biochemical factors underlying clot formation and dissolution in flowing blood*, J. of Theoretical Medicine, **5** (2003), 183–218.

[2] M. Anand, K. Rajagopal and K. R. Rajagopal, *A model for the formation, growth, and lysis of clots in quiescent plasma. A comparison between the effects of antithrombin III deficiency and protein C deficiency*, J. of Theoretical Biology, **253** (2008), 725–738.

[3] F. I. Ataullakhanov and M. A. Panteleev, *Mathematical modeling and computer simulation in blood coagulation*, Pathophysiol. Haemost. Thromb., **34** (2005), 60–70.

[4] S. P. Bhat and D. S. Bernstein, *Nontangency-based Lyapunov tests for convergence and stability in systems having a continuum of equilibria*, SIAM J. Control Optim., **42** (2003), 1745–1775.

[5] T. Bodnár and A. Sequeira, *Numerical simulation of the coagulation dynamics of blood*, Comp. Math. Methods in Medicine, **9** (2008), 83–104.

[6] I. Borsi, A. Farina, A. Fasano and K. R. Rajagopal, *Modelling the combined chemical and mechanical action for blood clotting*, In "Nonlinear Phenomena with Energy Dissipation," volume **29** of GAKUTO Internat. Ser. Math. Sci. Appl., pages 53–72. Gakkōtosho, Tokyo, 2008.

[7] S. L. Campbell and N. J. Rose, *Singular perturbations of autonomous linear systems*, SIAM Journal Math. Anal., **10** (1979), 542–551.

[8] M. H. Kroll, J. D. Hellums, L. V. McIntire, A. I. Schafer and J. L. Moake, *Platelets and shear stress*, Blood, **88** (1996), 1525–1541.

[9] A. L. Kuharsky and A. L. Fogelson, *Surface-mediated control of blood coagulation: The role of binding site densities and platelet deposition*, Biophys. J., **80** (2001), 1050–1074.

[10] A. Leuprecht and K. Perktold, *Computer simulation of non-Newtonian effects of blood flow in large arteries*, Computer Methods in Biomechanics and Biomech. Eng., **4** (2001), 149–163.

[11] L. Michaelis and M. L. Menten, *Die kinetik der invertinwirkung*, Biochem Z., **49** (1913), 333–369.

[12] Y. H. Qiao, J. L. Liu and Y. J. Zeng, *A kinetic model for simulation of blood coagulation and inhibition in the intrinsic path*, J. of Medical Eng. and Technology, **29** (2005), 70–74.

[13] A. M. Robertson, A. Sequeira and M. V. Kameneva, *Hemorheology*, In "Hemodynamical Flows: Modeling, Analysis and Simulation (Oberwolfach Seminars)," volume 37, G.P. Galdi, R. Rannacher, A. M. Robertson, and S. Turek (Eds.), Birkhäuser Verlag, 2008, 63–120.

[14] M. Schenone, B. C. Furie and B. Furie, *The blood coagulation cascade*, Curr. Opin. Hematol., **11** (2004), 272–277.

[15] L. A. Segel and M. Slemrod, *The quasy-steady-state assumption: A case study in perturbation*, SIAM Review, **32** (1989), 446–477.

[16] N. T. Wang and A. L. Fogelson, *Computational methods for continuum models of platelet aggregation*, J. Comput. Phys., **151** (1999), 649–675.

Received March 8, 2010; Accepted September 25, 2010.

E-mail address: adelia.sequeira@math.ist.utl.pt
E-mail address: rsantos@ualg.pt
E-mail address: bodnar@marian.fsik.cvut.cz